

Nickel(II) Complexes Bearing N,O-Chelate Ligands: Synthesis, Solid-Structure Characterization, and Reactivity toward the Polymerization of Polar Monomer

Xiaohui He,^{†,‡} Yingzheng Yao,[†] Xiang Luo,[†] Junkai Zhang,[†] Yunhai Liu,[†] Ling Zhang,[†] and Qing Wu^{*,†}

Institute of Polymer Science, Key Laboratory for Polymeric Composite and Functional Materials of the Ministry of Education, Zhongshan University, Guangzhou 510275, China, and The School of Environment and Chemical Engineering, Nanchang University, Nanchang 330029, China

Received April 22, 2003

Two new moisture- and air-stable bis(β -ketoamino)nickel(II) complexes Ni[R1C(O)CHC(NAr)R2]₂ (Ar \equiv 2,6-¹Pr₂C₆H₃; R1 = R2 = CH₃, **1**; R1 = C₆H₅, R2 = CH₃, **2**), together with the moderately stable complex Ni₂[CH₃C(O)CHC(O)CH₃]₄[H₂N^tBu]₂ (**3**), which bears a monoanionic O,O-chelate bidentate β -diketone and an sp³-N atom of ^tBuNH₂ mixed ligands, were synthesized and characterized. The solid-state structures of the complexes have been determined by single-crystal X-ray diffractions. Additionally, these new complexes act as catalyst precursors for methyl methacrylate polymerization after activation with methylaluminoxane (MAO). The polymers obtained by **1** and **2** show broader polydispersity than that obtained by **3**. ¹³C NMR analyses indicate that these catalytic systems initiate MMA polymerization to yield PMMA with rich syndiotacticity microstructure.

Introduction

The early transition metal complexes are difficult to handle and incompatible with polar monomers due to the high oxophilicity and the tendency for functionalities to coordinate to active species. Examples of vinyl polymerization of polar vinyl monomer are few.^{1,2} Some early transition metals have been shown to polymerize olefins with distant polar groups, but possibilities are limited.^{3–6} Late transition metal catalysts are less oxophilic than their early transition metals and potentially not poisoned by O-containing polar functionalities.^{7,8} In recent years there has been increasing interest in the development of late transition metal based complexes as catalysts for the polymerization of α -olefins and polar olefins.^{9–14} Ligands of the type O–Y (where Y is N or S) are particularly interesting and

subsequently interesting to mixed-ligand-complex catalytic systems, which are shown to be very effective catalysts in α -olefin and polar olefin polymerization, for example, nickel-based systems.^{15,16} The late transition metals can be stabilized by various heterodonor ligands and give mono- or dinuclear complexes with several coordination modes. In particular, complexes with two metal centers can catalyze the polar olefins more efficiently than analogous monometallic species. Therefore, bimetallic systems are of considerable interest. Although the late transition metals bearing β -ketoamines N,O mixed ligands and members of the general family have been extensively studied,^{17–19} only a few Ni(II) complexes containing analogous tetradentate β -ketoamines have been reported.^{20–24} The development

* Corresponding author. Fax: (086)-(20)-84112245. E-mail: ceswuq@zsu.edu.cn.

[†] Zhongshan University.

[‡] Nanchang University.

(1) Stehling, U. M.; Stein, K. M.; Kesti, M. R.; Waymouth, R. M. *Macromolecules* **1998**, *31*, 9679.

(2) Hennis, A. D.; Sen, A. *Polym. Prepr.* **2000**, *41* (2), 1383.

(3) Deng, H.; Soga, K. *Macromolecules* **1996**, *29*, 1847.

(4) Chung, T. C.; Rhubright, D. *Macromolecules* **1993**, *26*, 3019.

(5) Aaltonen, P.; Lofgren, B. *Macromolecules* **1995**, *28*, 5353.

(6) Yasuda, H.; Ihara, E. *Macromol. Chem. Phys.* **1995**, *196*, 2417.

(7) Recent reviews: (a) Brltovsek, G. J. P.; Gibson, V. C.; Wass, D. M. *Angew. Chem., Int. Ed.* **1999**, *38*, 428. (b) Itself, S. D.; Jhnsn, L. K.; Brookhart, M. *Chem. Rev.* **2000**, *100*, 1169. (c) Meking, S. *Coord. Chem. Rev.* **2000**, *203*, 325. (d) Meking, S. *Angew. Chem., Int. Ed.* **2001**, *40*, 534.

(8) New nickel(II) catalysts were recently developed by Bazan and co-workers and Brookhart, and co-workers: (a) Lee, B. Y.; Bazan, G. C.; Vela, J.; Komon, Z. J. A.; Bu, X. *J. Am. Chem. Soc.* **2001**, *123*, 5352. (b) Hicks, F. A.; Brookhart, M. *Organometallics* **2001**, *20*, 3217.

(9) Rix, F. C.; Brookhart, M. B.; White, P. S. *J. Am. Chem. Soc.* **1996**, *118*, 4746.

(10) Mecking, S.; Johnson, L. K.; Wang, L.; Brookhart, M. *J. Am. Chem. Soc.* **1998**, *120*, 888.

(11) Johnson, L. K.; Mecking, S.; Brookhart, M. *J. Am. Chem. Soc.* **1996**, *118*, 267.

(12) Brookhart, M.; Wagner, M. I. *J. Am. Chem. Soc.* **1996**, *118*, 7219.

(13) Wang, C.; Friedrich, S.; Younkin, T. R.; Li, R. T.; Grubbs, R. H.; Bansleben, D. A.; Day, M. W. *Organometallics* **1998**, *17*, 3149.

(14) Elia, C. N.; Sen, A.; Albeniz, A. C.; Espinet, P. *Proceedings of the ACS National Meeting*; Washington, August 20–24, 2000.

(15) Peukert, M.; Keim, W. *Organometallics* **1983**, *2*, 594.

(16) Reuben, B.; Wittcoff, H. *J. Chem. Educ.* **1988**, *65*, 605.

(17) Robards, K.; Patsalides, E.; Dilli, S. *J. Chromatogr.* **1987**, *411*, 1.

(18) (a) Everett, G. W., Jr.; Holm, R. H. *J. Am. Chem. Soc.* **1965**, *87*, 2117. (b) Everett, G. W., Jr.; Holm, R. H. *J. Am. Chem. Soc.* **1966**, *88*, 2442. (c) Everett, G. W., Jr.; Holm, R. H. *Inorg. Chem.* **1968**, *7*, 776. (d) Ernst, G. R. E.; O'Connor, M. J.; Holm, R. H. *J. Am. Chem. Soc.* **1967**, *89*, 6104.

(19) Veya, R.; Floriani, C.; Chiest-Villa, A.; Rizzoh, C. *Organometallics* **1993**, *12*, 4892.

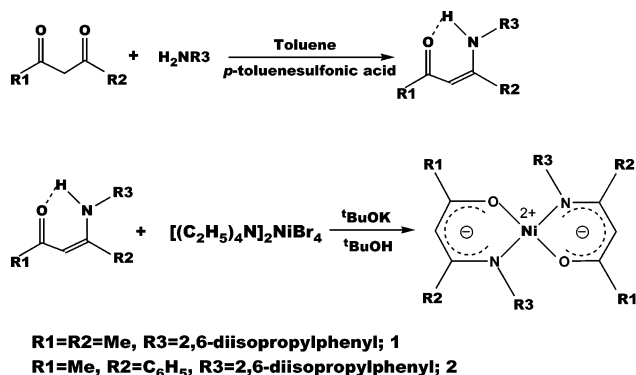
(20) Corazza, F.; Solari, E.; Floriani, C.; Chiesi-Villa, A.; Guastini, C. *J. Chem. Soc., Dalton Trans.* **1990**, 1335.

(21) Tjaden, E. B.; Swenson, D. C.; Jordan, R. F.; Petersen, J. L. *Organometallics* **1995**, *14*, 371.

(22) Floriani, C. *Polyhedron* **1989**, *8*, 1717.

(23) Mazzanti, M.; Rosset, J. M.; Floriani, C.; Chiesi-Villa, A.; Guastini, C. *J. Chem. Soc., Dalton Trans.* **1989**, 953.

Scheme 1



of new mixed-ligand Ni(II) complexes is important for the discovery of new late transition metal catalysts for α -olefin and polar olefin polymerization.

The fact that a little variation of the ligand structure may lead to profound changes in the catalytic reactivity prompted us to synthesize nickel catalysts chelated by various ligand frameworks containing N,O-chelate atoms. In this contribution, we report the syntheses and solid-structure characterizations of three new Ni(II) complexes with N,O-chelate mixed ligands. This is the first report on their syntheses and solid-structure characterizations and their application as catalyst precursors for methyl methacrylate polymerization after activation with methylaluminoxane (MAO).

Results and Discussion

β -Ketoamine Ligands and Bis(β -ketoamino)nickel(II) Complex Syntheses. Two N-aryl-substituted β -ketoamine ligands, 2-(2,6-diisopropylphenyl)amino-pent-2-en-4-one (**L1**) and 3-(2,6-diisopropylphenyl)amino-1-phenyl-but-2-en-4-one (**L2**), were synthesized by condensation of the corresponding acetylacetone (or benzoylacetone) and 2,6-diisopropylaniline by refluxing in toluene while removing water by a water separator. The further reaction of **L1** and **L2** with $[\text{Et}_4\text{N}]_2[\text{NiBr}_4]$ in the presence of a strong base, $^t\text{BuOK}$ and $^t\text{BuOH}$, afforded the corresponding bis(β -ketoamino)nickel(II) complexes **1** and **2** in moderate yields (as shown in Scheme 1).

The molecular structures were determined by single-crystal X-ray diffraction. The ORTEP plots are shown in Figures 1 and 2, respectively. Table 1 lists the selected bond lengths and angles. Crystallographic data are summarized in Table 2. The coordination geometries of both **1** and **2** were demonstrated to be very similar in the solid state and are *mononuclear* and nearly ideally *four-coordinate, square-planar* configurations. Interestingly, the anticipated formation of tetrahedral complexes, although sterically possible, was not observed either. The nickel atoms in both **1** and **2** are arranged in a nearly perfect square-planar coordination environment where the metal ion via β -ketoamine acts as a monoanionic bidentate N,O-chelator with N,O-donor atom sets and lies in the trans-configuration to create two stable six-membered metallacyclic chelate rings (NiOCCCN). The mean deviation of the metal center from the least-squares plane (CCNONiONCCC)

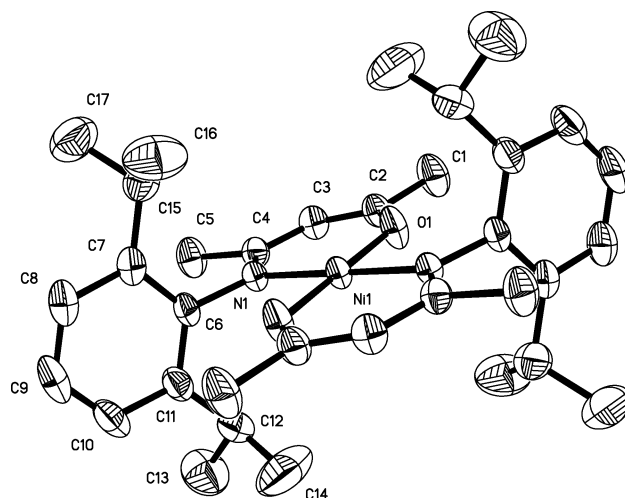


Figure 1. ORTEP plots of complex **1** showing the atom-labeling scheme. Hydrogen atoms are omitted for clarity.

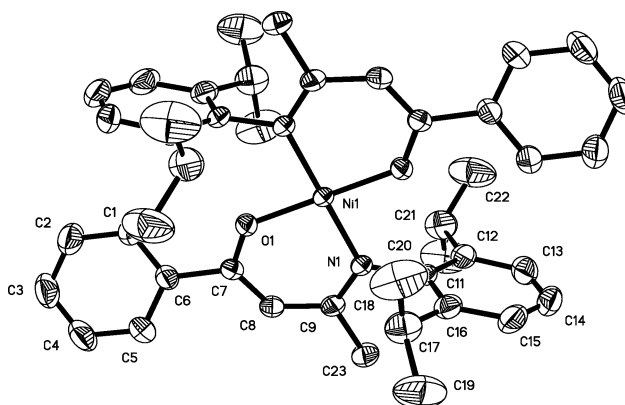


Figure 2. ORTEP plots of complex **2** showing the atom-labeling scheme. Hydrogen atoms are omitted for clarity.

is 0.0103 Å for **1** and 0.0567 Å for **2**. The bulky 2,6-diisopropylbenzene rings substituted on the imine moieties are satisfactorily planar with the mean deviation of 0.0048 Å for **1** and 0.0072 Å for **2**, respectively. They occupy the position trans and essentially perpendicular to the metallacycle plane. The phenyl ring unit attached to C instead of methyl in **2** is also quite planar (the mean deviation is 0.0025 Å); however, it swings slightly out of the previous metallacycle plane, forming an approximately 23.9° dihedral angle. The angles of O–Ni–O and N–Ni–N are all equal at 180.0° for both **1** and **2**. The N–Ni–O angles are slightly more than 90° (92.74(6)° in **1**, whereas 93.23(5)° in **2**). The O#1–Ni–N is slightly less than 90° (87.26(6)° for **1** and 86.77(5)° for **2**). An average metal–ligand bond length of Ni–O is 1.8177(13) Å for **1** and 1.8384(11) Å for **2**, and Ni–N is 1.9188(14) Å for **1** and 1.9300(13) Å for **2**, respectively.

Ni₂[CH₃C(O)CHC(O)CH₃]₄[H₂N^tBu]₂ (3**) Synthesis.** The attempt to prepare the β -ketoamine MeC(O)-CHC(N^tBu)Me ligand like **L1** and **L2** was unsuccessful using $^t\text{BuNH}_2$ instead of 2,6-diisopropylaniline. This is because the boiling point of $^t\text{BuNH}_2$ is very low, and the amine only reacts with acetylacetone directly rather than reacting by refluxing in toluene while removing water by a water separator, as in the preparation of **L1** and **L2**. Interestingly, a white solid product was obtained. Unfortunately, satisfactory elemental analysis, FAB-MS, and melting point cannot be obtained since

(24) Rosset, J. M.; Floriani, C.; Mazzanti, M. Chiesi-Villa, A.; Guastini, C. *Inorg. Chem.* **1990**, *29*, 3991.

Table 1. Selected Bond Lengths (Å) and Angles (deg) for Complexes 1, 2, and 3

1		2		3	
bond	length	bond	length	bond	length
Ni(1)–O(1)1	1.8177(13)	Ni(1)–O(1)	1.8384(11)	Ni(1)–O(1)	2.075(2)
Ni(1)–O(1)#1	1.8177(13)	Ni(1)–N(1)	1.9300(13)	Ni(1)–N(1)	2.116(5)
Ni(1)–N(1)	1.9188(14)	N(1)–O(1)#1	1.8384(11)	Ni(1)–O(2)	2.011(3)
Ni(1)–N(1)#1	1.9188(14)	Ni(1)–N(1)#1	1.9300(13)	Ni(1)–O(4)	1.999(2)
C(2)–O(1)	1.285(2)	O(1)–C(7)	1.2893(19)	Ni(1)–O(3)	2.027(2)
C(4)–N(1)	1.320(2)	C(9)–N(1)	1.323(2)	O(1)–C(2)	1.280(4)
C(6)–N(1)	1.444(2)	C(11)–N(1)	1.446(2)	C(2)–C(3)	1.380(5)
C(1)–C(2)	1.506(2)	C(9)–C(23)	1.511(2)	C(3)–C(4)	1.397(5)
C(2)–C(3)	1.362(3)	C(6)–C(7)	1.489(2)	C(4)–O(2)	1.250(4)
C(3)–C(4)	1.411(2)	C(7)–C(8)	1.368(2)	N(1)–C(11)	1.423(11)
C(4)–C(5)	1.513(2)	C(8)–C(9)	1.401(2)	O(4)–C(9)	1.269(4)
C(6)–C(11)	1.398(3)	C(16)–C(17)	1.515(3)	C(9)–C(8)	1.384(5)
C(11)–C(12)	1.516(3)	C(12)–C(21)	1.505(4)	C(8)–C(7)	1.390(5)
C(12)–C(13)	1.530(4)	C(17)–C(18)	1.523(4)	C(7)–O(3)	1.262(4)
C(12)–C(14)	1.504(5)	C(21)–C(22)	1.531(4)	Ni(1)–O(1)#1	2.156(2)
bond	angle	bond	angle	bond	angle
O(1)1–Ni(1)–N(1)1	92.74(6)	O(1)–Ni(1)–N(1)	93.23(5)	O(1)–Ni(1)–O(1)#1	79.65(9)
O(1)#1–Ni(1)–N(1)#1	92.74(6)	O(1)#1–Ni(1)–N(1)#1	93.23(5)	O(1)–Ni(1)–O(2)	91.17(10)
O(1)–Ni(1)–O(1)#1	180.0	O(1)#1–Ni(1)–O(1)	180.00(8)	O(2)–Ni(1)–O(4)	87.97(10)
N(1)#1–Ni(1)–N(1)	180.0	N(1)#1–Ni(1)–N(1)	180.00(8)	O(4)–Ni(1)–O(3)	90.65(10)
O(1)–Ni(1)–N(1)#1	87.26(6)	O(1)#1–Ni(1)–N(1)	86.77(5)	O(3)–Ni(1)–O(1)#1	88.88(10)
O(1)#1–Ni(1)–N(1)	87.26(6)	O(1)–Ni(1)–N(1)#1	86.77(5)	O(1)–Ni(1)–O(4)	178.93(8)
C(2)–O(1)–Ni(1)	130.14(12)	C(7)–O(1)–Ni(1)	128.63(11)	O(1)–Ni(1)–N(1)	81.07(17)
C(6)–N(1)–Ni(1)	117.25(11)	C(11)–N(1)–Ni(1)	120.55(10)	N(1)–Ni(1)–O(4)	98.28(17)
C(4)–N(1)–Ni(1)	125.63(12)	C(9)–N(1)–Ni(1)	124.41(11)	O(4)–Ni(1)–O(1)#1	101.22(10)
C(4)–N(1)–C(6)	117.12(14)	C(9)–N(1)–C(11)	115.01(13)	O(1)–Ni(1)–O(3)	89.99(9)
N(1)–C(4)–C(5)	120.41(16)	C(12)–C(11)–N(1)	119.43(17)	C(11)–N(1)–Ni(1)	134.2(7)
N(1)–C(4)–C(3)	123.40(16)	C(16)–C(11)–N(1)	118.63(16)	Ni(1)–O(1)–Ni(1)#1	100.35(9)
C(11)–C(6)–N(1)	118.62(16)	N(1)–C(9)–C(8)	123.74(15)	C(9)–O(4)–Ni(1)	124.5(2)
C(7)–C(6)–N(1)	118.96(16)	N(1)–C(9)–C(23)	121.06(16)	C(7)–O(3)–Ni(1)	123.7(2)
C(2)–C(3)–C(4)	123.64(17)	C(12)–C(11)–C(16)	121.90(17)	O(3)–Ni(1)–N(1)	164.6(3)
C(6)–C(11)–C(12)	121.90(17)	C(11)–C(16)–C(17)	121.17(17)	Ni(1)–O(1)–C(2)	123.0(2)
C(14)–C(12)–C(11)	111.6(3)	C(11)–C(12)–C(13)	116.9(2)	Ni(1)–O(2)–C(4)	125.3(2)
C(14)–C(12)–C(13)	110.4(3)	C(11)–C(12)–C(21)	122.21(18)	O(2)–Ni(1)–O(3)	90.12(11)
				N(1)–Ni(1)–O(1)#	89.91(18)
				O(2)–Ni(1)–N(1)	89.66(19)

Table 2. Crystallographic Data for Complexes 1, 2, and 3^a

	1	2	3
empirical formula	C ₃₄ H ₄₈ N ₂ NiO ₂	C ₄₄ H ₅₂ N ₂ NiO ₂	C ₂₈ H ₅₀ N ₂ Ni ₂ O ₈
fw	575.45	699.59	660.12
cryst color and form	dark brown	dark green	green
cryst syst	triclinic	monoclinic	triclinic
space group	<i>P</i> $\bar{1}$	<i>P</i> 2(1)/ <i>c</i>	<i>P</i> $\bar{1}$
<i>a</i> (Å)	8.5642(15)	11.2309(19)	9.073(5)
<i>b</i> (Å)	9.5979(17)	8.8805(15)	9.141(5)
<i>c</i> (Å)	11.260(2)	20.487(4)	11.513(6)
α (deg)	67.718(3)	90	110.555(9)
β (deg)	83.281(3)	107.707(3)	99.252(9)
γ (deg)	73.108(3)	90	100.637(9)
<i>V</i> (Å ³)	819.5(3)	1946.5(6)	851.9(8)
<i>Z</i>	1	2	1
<i>D</i> _c (Mg/m ³)	1.166	1.194	1.287
abs coeff μ (mm ⁻¹)	0.622	0.536	1.149
<i>F</i> (000)	310	748	352
cryst size (mm)	0.49 × 0.42 × 0.26	0.50 × 0.21 × 0.18	0.41 × 0.31 × 0.15
θ_{\max} (deg)	27.02	27.04	27.22
index ranges	–10 ≤ <i>h</i> ≤ 9 –12 ≤ <i>k</i> ≤ 12 –13 ≤ <i>l</i> ≤ 14	–14 ≤ <i>h</i> ≤ 13 –11 ≤ <i>k</i> ≤ 11 –15 ≤ <i>l</i> ≤ 26	–11 ≤ <i>h</i> ≤ 11 –11 ≤ <i>k</i> ≤ 10 –14 ≤ <i>l</i> ≤ 14
no. of params	178	223	191
goodness-of-fit on <i>S</i> (<i>F</i> ²) ^a	1.112	1.108	1.091
final <i>R</i> indices [<i>I</i> > 2 σ (<i>I</i>)]	0.0358; 0.1065	0.0359; 0.0987	0.0439; 0.1165
<i>R</i> indices (all data)	0.0375; 0.1082	0.0466; 0.1070	0.0597; 0.1288
largest diff peak and hole (e/Å ⁻³)	0.381, –0.311	0.373, –0.309	0.340, –0.488

$$^a R = \sum |F_o| - |F_c| / \sum |F_o|; R_w = [\sum w(F_o^2 - F_c^2)^2 / \sum w(F_o^2)]^{1/2}.$$

the solid is less stable at higher temperature and readily evaporates or decomposes by the external analytical conditions. However, the solid-state ¹³C NMR spectrum (see Figure 3) and the solution ¹³C and ¹H NMR spectra

of the product in CDCl₃ solvent (see Figure 4 and Figure 5, respectively) could be obtained. The solid-state ¹³C NMR spectrum is excellent, consistent with a simple acetylaceton ammonium salt, [tBuNH₃][acac] (**A**). The

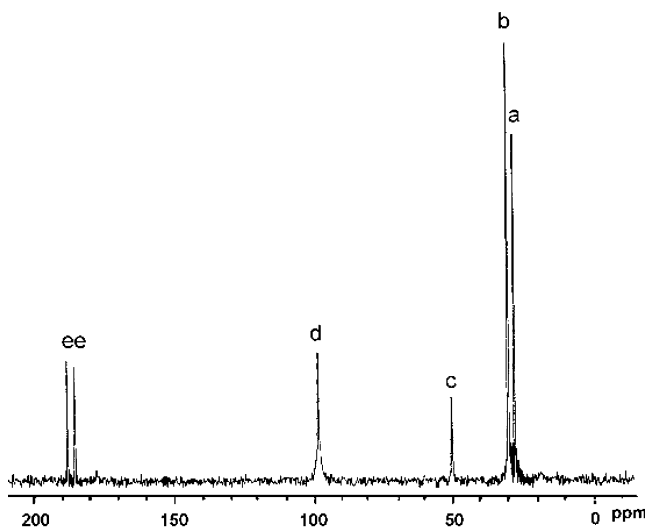


Figure 3. Spectrum of ^{13}C NMR of $[\text{tBuNH}_3][\text{acac}]$ (A) carried out on a Bruker AVANCE 400 Hz at room temperature in the solid state.

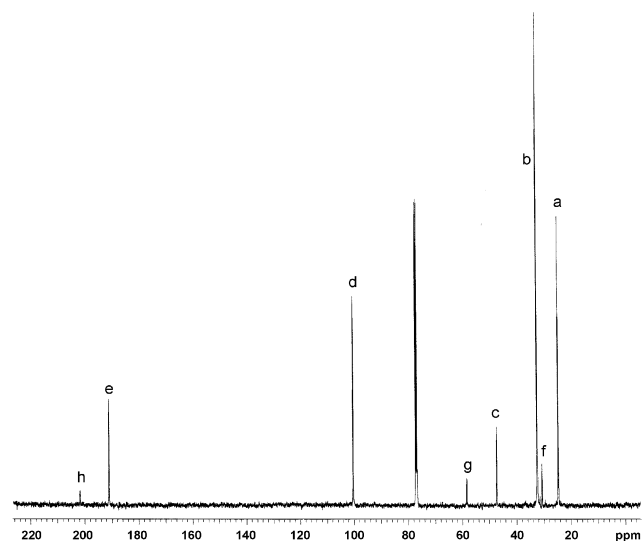


Figure 4. Spectrum of ^{13}C NMR of $[\text{tBuNH}_3][\text{acac}]$ (A + B) carried out on an INOVA 500 Hz at room temperature in CDCl_3 solution.

splitting carbonyl carbon resonance peaks (labeled e) apparently reflect that **A** has the cation H bonded to one oxygen of the acac anion and the charge of the acac anion is mainly concentrated on the oxygen within the solid lattice. Unlike the solid-state ^{13}C NMR spectrum, both solution ^{13}C and ^1H NMR spectra exhibit extra resonance peaks for another structure, **B**, besides the peaks for **A**, implying that $[\text{tBuNH}_3][\text{acac}]$ exists in equilibrium between the ionic form **A** and the H-bonded form **B** in polar solvent (as shown in Scheme 2, the ratio of **A**:**B** is about 6:1 calculated from both ^{13}C and ^1H NMR spectra). The unsplitting carbonyl carbon (labeled e) resonance peak of **A** in the solution ^{13}C spectrum reflects that the charge of the acac anion is more dispersed among the OCCCO field in solution. Therefore, $[\text{tBuNH}_3][\text{acac}]$ reacts with $[\text{Et}_4\text{N}]_2[\text{NiBr}_4]$ in the presence of $^t\text{BuOK}$ and $^t\text{BuOH}$ solvent to form the complex $\text{Ni}_2[\text{CH}_3\text{C}(\text{O})\text{CHC}(\text{O})\text{CH}_3]_4[\text{H}_2\text{N}^t\text{Bu}]_2$ (**3**), although following procedures similar to the preparation of complexes **1** and **2**. This is because the $[\text{acac}]^-$ of $[\text{t}$

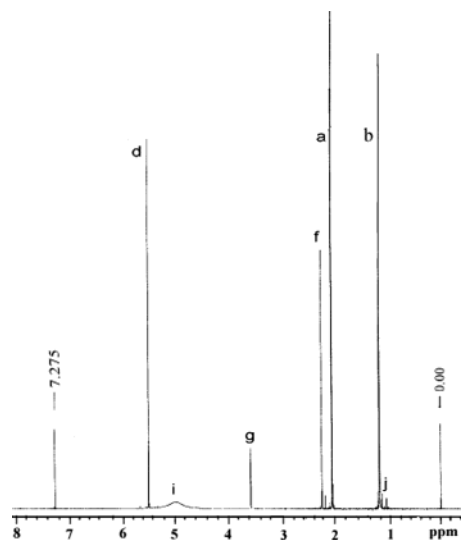
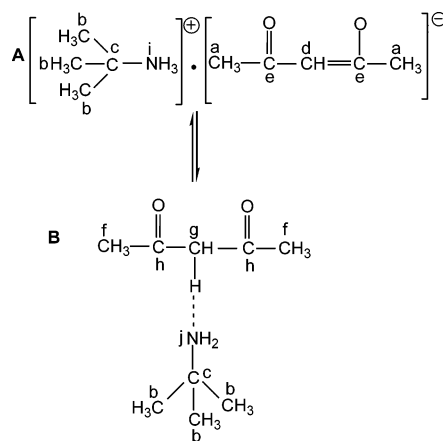


Figure 5. Spectrum of ^1H NMR of $[\text{tBuNH}_3][\text{acac}]$ (A + B) carried out on an INOVA 500 Hz at room temperature in CDCl_3 solution and using TMS as internal standard.

Scheme 2



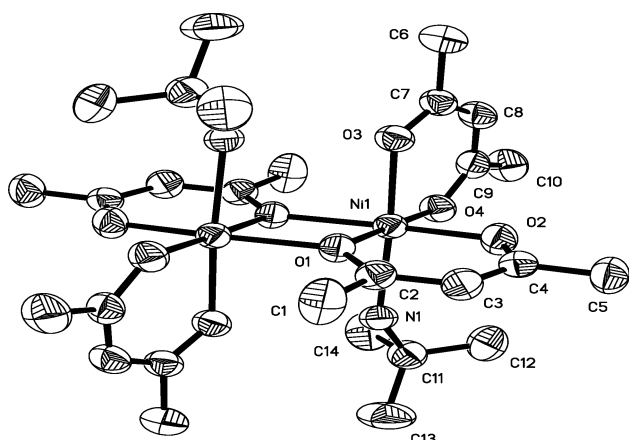
$\text{BuNH}_3][\text{acac}]$ can stably exist in the presence of $^t\text{BuOH}$ solvent and can coordinate directly to the Ni ion, and the remaining acac and $[\text{tBuNH}_3]^+$ were further deprotonated by the strong base $^t\text{BuOK}$ to form the corresponding $[\text{acac}]^-$ and $^t\text{BuNH}_2$ and then further coordinated to the Ni ion to give the resulting nickel(II) complex with β -diketonate monoanions and the $\text{sp}^3\text{-N}$ atom of $^t\text{BuNH}_2$ mixed ligands.

Crystallographic analysis of **3** (as shown in Figure 6) reveals the molecular structure is a *binuclear* and *six-coordinate, pseudo-octahedral* geometric coordination sphere around the nickel center, in which one β -diketonato is a monoanionic bidentate O,O-chelator with O,O-donor atoms sets, while another O,O-ligand, besides acting as a terminal oxygen coordination, also acts as a bridging oxygen coordinator between two metal centers, forming a binuclear structure. In each nickel(II) center, five positions were occupied by one β -diketonato anion bidentate ligand, a bridging oxygen, and the terminal oxygen atoms of another β -diketonato anion, respectively. The sixth coordination position is occupied by a $\text{sp}^3\text{-N}$ atom of $^t\text{BuNH}_2$, which is located at the position trans to the terminal oxygen atom of the O,O-donor atom sets with a nearly linear N–Ni–O angle ($164.6(3)^\circ$), to complete a slight distorted octahedral geometry around the metal center. The entire Ni_2O_6

Table 3. Methyl Methacrylate Polymerization with Catalysts 1–3/MAO^a

entry	catalyst	T_p (°C) ^b	act. ^c	M_w ($\times 10^{-5}$) ^d	M_w/M_n	mm (%) ^e	mr (%) ^e	rr (%) ^e
1	1	0	1.20	0.38	2.33	n.d.	n.d.	n.d.
2	1	25	3.59	0.65	2.64	n.d.	n.d.	n.d.
3	1	50	18.6	0.83	4.34	7.6	33.4	59.0
4	1	70	9.54	1.45	6.01	n.d.	n.d.	n.d.
5	2	0	0.75	0.42	2.46	n.d.	n.d.	n.d.
6	2	25	1.33	0.60	2.93	n.d.	n.d.	n.d.
7	2	50	7.65	0.74	5.64	n.d.	n.d.	n.d.
8	2	70	4.89	1.54	6.07	n.d.	n.d.	n.d.
9	3	0	12.0	0.94	1.56	n.d.	n.d.	n.d.
10	3	25	279.4	1.07	1.44	0.5	17.2	82.3
11	3	50	327.4	1.16	1.41	n.d.	n.d.	n.d.
12	3	70	125.1	1.09	1.47	n.d.	n.d.	n.d.

^a Ni = 5×10^{-3} mmol; MMA = 0.05 mol; t_p = 7 h (for **1** and **2**); Ni = 5.56×10^{-3} mmol; MMA = 0.05 mol; t_p = 1 h (for **3**). ^b Polymerization temperature. ^c Activity in kg polymer (mol catalyst h)⁻¹. ^d Solvent: chloroform; temperature: 40 °C; M_w are the relative weight-average molecular weights; calibration with polystyrene standards. ^e Tacticity determined by ¹³C NMR. n.d. = not determined.

**Figure 6.** ORTEP plot of complex **3** showing the atom-labeling scheme. Hydrogen atoms are omitted for clarity.

portion of the molecule has a small deviation of 0.010 Å, and both nickel ions are essentially in the Ni₂O₆ plane with Ni(1) displaced by +0.0023 Å and Ni(1)# by -0.0023 Å from the plane of its ligands. The mean deviation of the NiOCCCO plane is 0.0584 Å, and that of another NiOCCCO plane is 0.0788 Å, with a 91.6° swing angle. The O–Ni–O angles average 87.664°, in the range from 79.65(9°) to 91.17(10°). The O–Ni–N angles of the nitrogen atom of the ^tBuNH₂ ligand also average 89.675°, although the range is greater, from 81.07(17°) to 98.28(17°). Four C–O bond lengths are almost the same (av 1.2605(4) Å), and the five Ni–O bond lengths are roughly equivalent (av 2.0536(2) Å). The Ni(1)–N(1) bond length is equal to 2.116(5) Å and N(1)–C(11) is 1.423(11) Å. A longer Ni(1)⋯Ni(1)# separation (the Ni–Ni distance is 3.250 Å) suggests that there is no Ni–Ni interaction between the metal ions. This is also reflected in the fairly large Ni–O_b–Ni angles (O_b and O_t = bridging and terminal oxygen atoms, respectively) of 100.35(9°).

Polymerization of MMA. All of the complexes can be activated with MAO to catalyze MMA polymerization. The polymers were isolated as white solids and characterized by GPC in chloroform using standard polystyrene as the reference. The triad microstructure of the PMMA was analyzed using ¹³C NMR spectroscopy. The results of polymerizations are summarized in Table 3. The activity of **3** is higher, while those of **1** and **2** are only moderate, and all increase in activity with increasing reaction temperature. The highest catalytic activities are obtained at 50 °C, but decrease signifi-

cantly as the temperature is increased to 70 °C. The polymers obtained by **1** and **2** show broader polydispersity than that obtained by **3**. The results of PMMA stereotriad distributions with [rr] = 59.0%, [mr] = 33.4%, [mm] = 7.6% (entry 3), and [rr] = 82.3%, [mr] = 17.20%, [mm] = 0.5% (entry 10) indicated that these catalytic systems initiate MMA polymerization to yield PMMA with rich syndiotacticity microstructure.

Experimental Section

General Procedures and Materials. All manipulations involving air- and moisture-sensitive compounds were carried out under an atmosphere of dried and purified nitrogen using standard Schlenk techniques. Solvents were purified using standard procedures. Benzoylacetone (98%) and 2,6-diisopropylphenylamine (90%) were obtained from Aldrich and used without further purification. **L1** and **L2** were synthesized by condensation of the corresponding acetylacetone (or benzoylacetone) and 2,6-diisopropylaniline following published procedures with minor modifications.^{25–27} [tBuNH₃][acac] (**A**) was synthesized by the direct reaction of acetylacetone with ^tBuNH₂. [Et₃N]₂[NiBr₄] was prepared according to the literature.²⁸ The Ni(II) complexes were synthesized according to the modified procedure of analogous Ni(II) complexes reported by Holm and co-workers.¹⁸ MMA was purified by drying from CaH₂ and distilling under vacuum (42 °C/70 mmHg) and dissolved in toluene to make a 5.0 mol/L solution. Elemental analyses were performed on a Vario EL microanalyzer. Mass spectra were measured on a VG ZAB-HS instrument using fast atom bombardment (FAB). NMR spectra were carried out on an INOVA 500 Hz at room temperature in CDCl₃ solution (using TMS as internal standard for ¹H NMR) and on a Bruker AVANCE 400 Hz at room temperature in the solid state (using a glycine standard sample spectrum to calibrate). Gel permeation chromatography (GPC) analyses of the molecular weight and molecular weight distribution of the polymers were performed on a Waters 150C instrument using standard polystyrene as the reference and with chloroform as the eluent at 40 °C. Melting points were recorded on a Tormas model 40 micro hot stage and are uncorrected.

[CH₃C(O)CHC(HNAr)CH₃] (**L1**, Ar = 2,6-ⁱPr₂C₆H₃). Acetylacetone (15 mL, 0.143 mol), 2,6-diisopropylphenylamine (30 mL, 0.143 mol), and a catalytic amount of *p*-toluenesulfonic acid in toluene (150 mL) were combined and heated to reflux

(25) Martin, D. F.; Janusonis, G. A.; Martin, B. B. *J. Am. Chem. Soc.* **1961**, *83*, 73.

(26) Martin, D. F. In *Reactions of Coordinated Ligands and Homogeneous Catalysis*; Advances in Chemistry Series, No. 37; American Chemical Society: Washington, DC, 1963; p 192–200.

(27) Clegg, W.; Cope, E. K.; Edwards, A. J.; Mair, F. S. *Inorg. Chem.* **1998**, *37*, 2317.

(28) Giil, N. S.; Nyholm, R. S. *J. Chem. Soc.* **1959**, 3997.

for 2–3 h, while H₂O was removed as a toluene azeotrope at 125–130 °C using a water separator. Vacuum distillation and recrystallization from hexane yielded 2-(2,6-diisopropylphenyl)aminopent-2-en-4-one (21.4 g, 56.5%, based on initial amount of acetylacetone (lit. 22.23 g, 58.7%)). Mp: 46.05 °C (lit. 44–46 °C). Anal. Calcd for C₁₇H₂₅NO: C, 78.72; H, 9.72; N, 5.40. Found: C, 79.05; H, 9.60; N, 5.26. Positive FAB-MS (*m/z*): 260 (M + 1); 244 (M – CH₃); 202 (M – CH₃C(O)CH). ¹H NMR (CDCl₃), δ (ppm): 12.1 (s, 1H, –NH); 7.2–7.3 (3H, –C₆H₃(Pr)₂); 5.2 (s, 1H, CH₃C(O)CH=); 3.0 (2H, 2 –CH(CH₃)₂); 2.1 (s, 3H, CH₃C(O)–); 1.6 (s, 3H, –CH₃); 1.1–1.2 (d, 12H, 2 –CH(CH₃)₂). ¹³C NMR (CDCl₃), δ (ppm): 195.8, 163.3, 146.2, 133.5, 128.2, 123.5, 95.5, 29.0, 28.4, 24.5, 22.6, 19.1.

[C₆H₅C(O)CHC(HNAr)CH₃] (L₂). 3-(2,6-Diisopropylphenyl)imino-1-phenylbut-2-en-1-one (**L₂**) was obtained as white crystals by using a procedure similar to that described for the synthesis of **L₁**, using 2,6-diisopropylphenylamine (13 mL, 0.062 mol), benzoylacetone (10 g, 0.060 mol), and a catalytic amount of *p*-toluenesulfonic acid in toluene (80 mL). Yield: 8.654 g, 44.61%, based on initial amount of benzoylacetone. Mp: 109.6 °C. Anal. Calcd for C₂₂H₂₇NO: C, 82.20; H, 8.47; N, 4.36. Found: C, 82.24; H, 8.28; N, 4.14. FAB-MS (*m/z*): 322 (M + 1); 306 (M – CH₃); 202 (M – C₆H₅C(O)CH); 105 (M – CH₃(HNAr)CCH). ¹H NMR (CDCl₃), δ (ppm): 12.8 (s, 1H, –NH); 8.0 (2H, C₆H₅C(O)–); 7.2–7.3 (2H, –HNC₆H₃(Pr)₂); 7.3–7.5 (4H, C₆H₅C(O)CHC(HNC₆H₃(Pr)₂)CH₃); 6.4 (s, 1H, C₆H₅C(O)CH=); 3.1 (2H, –(CH₃)₂); 1.8 (s, 3H, CH₃); 1.2 (d, 12H, 2 –CH(CH₃)₂). ¹³C NMR (CDCl₃), δ (ppm): 188.4, 165.2, 146.2, 140.0, 133.5, 132.2, 130.7, 128.6, 128.4, 128.2, 127.1, 127.0, 124.2, 123.6, 92.1, 28.5, 28.3, 24.6, 22.7, 19.7.

[^tBuNH₂][acac] (A). A white needle crystal formed immediately when 20 mL (0.20 mol) of ^tBuNH₂ was introduced slowly into 21 mL (0.2002 mol) of acetylacetone without a large amount of heating. Filtering isolated the crude product. The purified product was obtained with a yield of 84% by further washing with approximately 20 mL of hexane several times and drying at 0 °C. ¹³C NMR (solid state), δ (ppm): 27.7 (CH₃C(O)CHC(O)CH₃(a)); 30.6 ((CH₃)₃CNH₃(b)); 50.8 ((CH₃)₃CNH₃(c)); 98.5 (CH₃C(O)CHC(O)CH₃(g)); 185.9, 188.6 (CH₃C(O)CHC(O)CH₃(e)). ¹H NMR (CDCl₃), δ (ppm): 1.0 ((CH₃)₃CNH₂(j)); 1.1 ((CH₃)₃CNH₃(b)); 2.0 (CH₃C(O)CHC(O)CH₃(a)); 2.2 (CH₃C(O)CH₂C(O)CH₃(f)); 3.6 (CH₃C(O)CH₂C(O)CH₃(g)); 5.0 ((CH₃)₃CNH₃(i)); 5.5 (CH₃C(O)CHC(O)CH₃(d)). ¹³C NMR (CDCl₃), δ (ppm): 24.6 (CH₃C(O)CHC(O)CH₃(a)); 30.6 (CH₃C(O)CH₂C(O)CH₃(f)); 32.3 ((CH₃)₃CNH₃(b)); 47.1 ((CH₃)₃CNH₃(c)); 58.4 (CH₃C(O)CH₂C(O)CH₃(f)); 100.2 (CH₃C(O)CHC(O)CH₃(g)); 190.9 (CH₃C(O)CHC(O)CH₃(e)); 201.7 (CH₃C(O)CH₂C(O)CH₃(h)).

Ni[CH₃C(O)CHC(NAr)CH₃]₂ (1). A 0.293 g (0.007 mol) sample of potassium was added to 25 mL of dried ^tBuOH. After the potassium had dissolved completely, the solution was heated to 50 °C and 1.950 g (0.0075 mol) of **L₁** added. The solution changed to yellow-orange as **L₁** completely reacted with ^tBuOK and was kept stirring for 20 min. The solution was cooled slowly to room temperature, and 2.320 g (0.0038 mol) of [Et₄N]₂[NiBr₄] was introduced in; the reacting mixture immediately formed a gray-green precipitate. After it was stirred vigorously at room temperature for several hours, the residual ^tBuOH was removed by evaporating in vacuum. The residue slurry was then extracted successively with enough hot *n*-heptane/toluene, the filtrate was collected by fast hot filtering, and the resulting hot filtrate was induced to crystallize by cooling slowly overnight. Then the product was isolated by filtering and drying under reduced pressure. One or two further recrystallizations from *n*-heptane/toluene mixture solution can result in dark brown block crystals. Yield: 0.997

g, 45.6%. Mp: 236 °C (dec). Anal. Calcd for C₃₄H₄₈N₂NiO₂: C, 75.54; H, 7.49; N, 4.00. Found: C, 75.34; H, 7.64; N, 3.95. ¹H NMR (CDCl₃), δ (ppm): 7.0–7.1 (3H, –C₆H₅(CH(CH₃)₂)); 4.8 (s, 1H, CH₃C(O)CH=); 3.8 (2H, 2 –CH(CH₃)₂); 1.6 (d, 6H, –CH(CH₃)₂); 1.4 (s, 3H, CH₃C(O)–); 1.2 (d, 6H, –CH(CH₃)₂); 0.9 (s, 3H, –CH₃). ¹³C NMR (CDCl₃), δ (ppm): 174.5, 165.3, 144.4, 142.0, 124.6, 122.6, 97.7, 28.3, 24.2, 24.1, 23.7, 22.2.

Ni[C₆H₅C(O)CHC(NAr)CH₃]₂ (2). Ni(II) complex **2** (as dark green block crystals) was obtained analogously to the preparation of **1**: 0.260 g (0.0065 mol) of potassium, 22 mL of dried ^tBuOH, 2.02 g (0.0063 mol) of **L₂**, and 2.271 g (0.0037 mol) of [Et₄N]₂[NiBr₄]. Yield: 1.140 g, 46.1%. Mp: 262 °C (dec). Anal. Calcd for C₄₄H₅₂N₂NiO₂: C, 70.96; H, 8.41; N, 4.87. Found: C, 69.86; H, 8.48; N, 4.75. ¹H NMR (CDCl₃), δ (ppm): 7.0–7.3 (6H, C₆H₅C(O)CH(NC₆H₅(CH(CH₃)₂)₂)CH₃); 6.3 (2H, C₆H₅C(O)–); 5.5 (s, 1H, C₆H₅C(O)CH=); 4.3 (2H, –CH(CH₃)₂); 1.5 (s, 3H, –CH₃); 1.3 (d, 12H, 2 –CH(CH₃)₂). ¹³C NMR (CDCl₃), δ (ppm): 170.0, 166.6, 144.9, 142.5, 136.8, 128.7, 127.1, 126.5, 125.1, 97.3, 28.6, 25.2, 24.0, 23.7.

Ni₂[CH₃C(O)CHC(O)CH₃]₄[H₂N⁺Bu]₂ (3). Ni(II) complex **3** (as green block crystals) was obtained by following procedures similar to those for the preparation of **1** and **2**: 0.294 g (0.007 mol) of potassium, 25 mL of dried ^tBuOH, 1.998 g (0.011 mol) of **A**, and 3.056 g (0.005 mol) of [Et₄N]₂[NiBr₄]. Yield: 0.672 g, 40.7%. Anal. Calcd For C₂₈H₅₀N₂Ni₂O₈: C, 50.95; H, 7.64; N, 4.22. Found: C, 50.88; H, 7.59; N, 4.14. The melting point was not obtained above 310 °C.

Polymerization Experiment. The appropriate MAO solid was introduced into the round-bottom glass flask, then toluene (15 mL), an appropriate amount of Ni(II) complex solution, and 10 mL of MMA (0.05 mol) were syringed into the well-stirred solution in order, and the reaction was continuously stirred for an appropriate period at polymerization temperature. Polymerizations were stopped by addition of the acidic EtOH. The resulting precipitated PMMA was collected and treated by filtering, washing with EtOH several times, and drying in vacuum at 60 °C to a constant weight.

Crystal Structure Determination. The crystals were mounted on a glass fiber using the oil drop scan method.²⁹ Data obtained with the ω–2θ scan mode were collected on a Bruker SMART 1000 CCD diffractometer with graphite-monochromated Mo Kα radiation (λ = 0.71073 Å) at 293 K. The structures were solved using direct methods, while further refinement with full-matrix least squares on F² was obtained with the SHELXTL program package.^{30,31} All non-hydrogen atoms were refined anisotropically. Hydrogen atoms were introduced in calculated positions with the displacement factors of the host carbon atoms.

Acknowledgment. This work was financially supported by the National Natural Science Foundation of China and the Science Foundation of Guangdong Province. The authors thank Mr. Feng for single-crystal X-ray technical assistance.

Supporting Information Available: Tables and figures giving X-ray crystallographic details for **1**, **2**, and **3** in CIF format. This material is available free of charge via the Internet at <http://pubs.acs.org>.

OM030292N

(29) Kottke, T.; Stalke, D. *J. Appl. Crystallogr.* **1993**, *26*, 615.

(30) SHELXTL, Version 5.1; Bruker AXS: Madison, WI, 1998.

(31) Sheldrick, G. M. SHELXL-97, program for X-ray Crystal Structure Solution and Refinement; Göttingen University: Germany, 1998.